Tunable magnetic properties and magnetocaloric effect of TmGa by Ho substitution

S. X. Yang,[1,2] X. Q. Zheng,[1,*] W. Y. Yang,[3] J. W. Xu,[1] J. Liu,[2] L. Xi,[1] H. Zhang,[1] L. C. Wang,[4,5] Z. Y. Xu,[2,4] J. Y. Zhang,[1] Y. F. Wu,[1] X. B. Ma,[6] D. F. Chen,[6] J. B. Yang,[3] S. G. Wang,[1,†] and B. G. Shen[2,1,4,‡]

[1]*School of Materials Science and Engineering, Beijing Advanced Innovation Center for Materials Genome Engineering, University of Science and Technology Beijing, Beijing 100083, China*

[2]*Beijing National Laboratory for Condensed Matter Physics, Institute of Physics, Chinese Academy of Sciences & University of Chinese Academy of Sciences, Beijing 100190, China*

[3]*State Key Laboratory for Mesoscopic Physics, School of Physics, Peking University, Beijing 100871, China*

[4]*Institute of Rare Earths, Chinese Academy of Sciences, Jiangxi 341000, China*

[5]*Key Laboratory of Cryogenics, Technical Institute of Physics and Chemistry, Chinese Academy of Sciences, Beijing 100190, China*

[6]*Department of Nuclear Physics, China Institute of Atomic Energy, Beijing 102413, China*

(Received 14 February 2020; revised 28 September 2020; accepted 28 October 2020; published 30 November 2020)

The influence of Ho substitution for Tm atoms on the magnetic properties and magnetocaloric effect (MCE) of TmGa compound was systematically investigated according to magnetic measurements and neutron powder diffraction (NPD) experiments. The magnetic transitions of $Tm_{1-x}Ho_xGa$ compounds show different types by Ho substitution due to the variation of spin and orbital angular momentum quantum number and the complete magnetic diagram of $Tm_{1-x}Ho_xGa$ compounds was obtained. The spin reorientation (SR) transition of $Tm_{0.1}Ho_{0.9}Ga$ compound was directly confirmed by variable-temperature NPD experiments. Results show that the magnetic moment orders along the c axis at the temperatures between T_{SR} and T_C and it cants away from the c axis towards the ab plane upon cooling below T_{SR}. Furthermore, Ho substitution plays a dominant role in MCE of $Tm_{1-x}Ho_xGa$ compounds. When $x = 0.15$, the peak value of magnetic entropy change reaches the maximum value of 18.0 J/kg K under field change of 0–2 T. The refrigerant temperature span (δT_{FWHM}) and refrigeration capacity of $Tm_{0.85}Ho_{0.15}Ga$ compound show enhancement of 23.0 and 21.6%, correspondingly, compared with TmGa compound. The giant MCE of $Tm_{0.85}Ho_{0.15}Ga$ compound results from the optimization of spin and total angular momentum quantum number by Ho substitution.

DOI: 10.1103/PhysRevB.102.174441

I. INTRODUCTION

Magnetocaloric effect (MCE) is one of the intrinsic physical properties of magnetic materials during the process of magnetic transitions. A mass of magnetic materials with large MCE have drawn much attention not only because of the interesting physical mechanism but also because of the potential applications on magnetic refrigeration [1–8]. Especially, MCE materials with low transition temperatures are presumably used for low-temperature refrigeration such as gas liquefaction [9–12]. In general, MCE materials are evaluated by magnetic entropy change (ΔS_M), refrigeration capacity (RC), refrigerant temperature span (δT_{FWHM}), together with adiabatic temperature change (ΔT_{ad}). Magnetic transitions and specific form of magnetic structure have important influence on the performance of MCE and there are abundant physics behind them. In the past decades, much work has been done to optimize magnetic transitions and balance the MCE parameters, where manipulating spin (S) and orbital angular momentum quantum number (L) of magnetic atoms has been proved to be effective [13,14].

Rare-earth based intermetallic compounds exhibit abundant magnetic properties and complex magnetic transitions [15–18]. Most of RGa (R = rare earth) compounds undergo two magnetic transitions with increasing temperature: spin reorientation (SR) and ferromagnetic (FM) to paramagnetic (PM) transition according to Mössbauer spectroscopy and neutron diffraction experiments [19–22]. According to magnetization and susceptibility measurements, the Curie temperatures of RGa (R = Gd, Tb, Dy, Ho, Er) compounds were determined to be 183, 158, 116, 63, and 32 K, respectively [23]. The transition temperatures for SR were determined to be 66, 31, 25, 20, and 15 K, correspondingly [24]. The Gd moments in GdGa compound are FM ordered along the b axis below T_C and they rotate away the b axis in the bc plane into two groups with different intersection angles with further increasing temperature below T_{SR} [20]. TbGa, DyGa, and HoGa compounds are simple ferromagnets with c axis as the easy direction of magnetization. Specifically, the Dy sublattice in DyGa compound is FM-ordered c axis below T_C and the Dy magnetic moments cant away from the c axis towards the a axis upon cooling below T_{SR} [21]. The magnetic transitions of HoGa compound was investigated in detail and large magnetic entropy change was reported [25].

*zhengxq@ustb.edu.cn
†sgwang@ustb.edu.cn
‡shenbg@iphy.ac.cn

Neutron diffraction experiments show that Ho sublattice is ferromagnetic along the c axis below T_C and Ho moments cant away from the c axis towards the ab plane upon cooling below T_{SR} [22]. ErGa compound was reported to undergo an SR transition with easy magnetization direction rotating from bc plane to a axis with decreasing temperature [19]. TmGa compound shows more complex magnetic transitions and lower transition temperatures. It was found that TmGa experiences an FM to antiferromagnetic (AFM) transition at T_{FA} and an AFM to PM transition at T_N with increasing temperature [26]. The easy magnetization direction of TmGa is along the a axis and the initial magnetic ordering with an incommensurate antiferromagnetic structure occurs at T_N. A simple collinear FM component together with a weak incommensurate component was observed with further decreasing temperature below T_{FA} [27]. Most RGa compounds show large magnetic entropy change and multiple peaks on MCE curves [24]. Especially, TmGa shows the largest MCE among RGa compounds at low temperatures with $(-\Delta S_M)_{max}$ of 20.6 J/kg K under field change of 0–2 T compared with ErGa (10.9 J/kg K). However, the value of RC is only 149.0 J/kg for TmGa, which is much smaller than that of ErGa (166.0 J/kg) [26,28]. Therefore, it is necessary to balance the parameters including ΔS_M, RC, and δT_{FWHM} for further applications and further understand the related physical mechanism behind it. In this work, the spin and total angular momentum quantum number of TmGa were optimized by substituting Ho atoms for Tm atoms. The tunable magnetic transitions and MCEs of $Tm_{1-x}Ho_xGa$ compounds were systematically investigated.

II. EXPERIMENTAL DETAILS

A series of polycrystalline $Tm_{1-x}Ho_xGa$ ($0 \leqslant x \leqslant 1$) compounds were synthesized by arc-melting method in argon atmosphere. Considering of the volatilization, 2% of Ho and Tm was over added into the stoichiometric amounts of mixture before melting. The purity of the starting elements is higher than 99.9%. The ingots were turned over several times to ensure the homogeneity. The samples were annealed at 1073 K for 7 d, and a subsequent quenching in liquid nitrogen was performed. The annealed samples were ground into powder and the purity together with crystal structure were examined by powder x-ray-diffraction (XRD) experiments with Cu-Kα radiation (wavelength $\lambda = 1.5406$ Å). The neutron diffraction patterns were collected using the high-intensity powder diffractometer at the China Advanced Research Reactor with an incident neutron wavelength of 1.478 Å. The Rietveld refinement analysis was performed by using the programs of GSAS and FULLPROF. Thermal magnetization and isothermal magnetization curves were measured on the Quantum-designed vibrating sample magnetometer. Furthermore, demagnetization with oscillation mode was performed before isothermal magnetic measurements to eliminate the influence of remanence.

III. RESULTS AND DISCUSSION

The powder XRD data of all the samples measured at room temperature were analyzed by the Rietveld refinement method. The experimental XRD pattern together with fitting pattern of $Tm_{0.4}Ho_{0.6}Ga$ compound is shown in Fig. 1(a). It can be seen that the $Tm_{0.4}Ho_{0.6}Ga$ compound is pure phase because all the peaks can be indexed to the Bragg positions of referenced structure. Further analysis indicates that $Tm_{0.4}Ho_{0.6}Ga$ compound has the orthorhombic CrB-type structure (space group $Cmcm$), which is in good accordance with reported results [19,26]. The rare-earth and Ga atoms occupy two different 4c sites with the same site symmetry (m 2 m) but different coordinates. The lattice parameters a, b, and c were determined to be 4.2663(1), 10.7484(2), and 4.0364(1) Å, respectively. The crystal structure is presented in the inset of Fig. 1(a). Other $Tm_{1-x}Ho_xGa$ compounds have the similar results with $Tm_{0.4}Ho_{0.6}Ga$. In order to investigate the variation of lattice constant with Ho content in detail, the contour plots of XRD intensity in a partial range of diffraction angle are shown in Fig. 1(b). It can be clearly seen that the positions of peak (111), (130), and (040) all move towards lower degrees with the increasing Ho content, indicating that lattice expansion occurs according to the Bragg equation. Moreover, Ho-content dependences of lattice parameters a, b, and c for $Tm_{1-x}Ho_xGa$ ($0 \leqslant x \leqslant 1$) compounds were all calculated and plotted in Figs. 1(c)–1(e), respectively. Monotonically increasing trend and nearly linear relationship between lattice parameters and Ho content were found, which arises from the fact that Ho atoms have larger radius than Tm atoms. The above results also show that Ho substitution makes no changes on the crystal structure and symmetry but only on the detailed lattice parameters.

Zero field-cooling (ZFC) and field-cooling (FC) data were collected with an applied field of 0.01 T to investigate the magnetic transitions of $Tm_{1-x}Ho_xGa$ ($0 \leqslant x \leqslant 1$) compounds. It was found that more than one obvious change can be observed clearly from the thermal magnetization (MT) curves indicating that complex magnetic transitions exist in $Tm_{1-x}Ho_xGa$ ($0 \leqslant x \leqslant 1$) compounds. According to previous results on TmGa and HoGa compounds [22,25–27], the change at high temperatures corresponds to the order to disorder transition which includes AFM to PM transition at T_N or FM to PM transition at T_C. With increasing Ho content from 0 to 1, the order to disorder transition temperature increases from 15.6 to 66.5 K as presented in Table I, indicating that Ho substitution has a large influence on magnetic ordering in $Tm_{1-x}Ho_xGa$ compounds. In fact, the order to disorder transition originates from the competition between magnetic exchange interaction and thermal vibration. For rare-earth based intermetallic compounds, the magnetic exchange interaction is positively correlated with spins. Since the spin angular momentum quantum number of Ho is larger than that of Tm, Ho substitution improves the average spin, and finally results in the increasing transition temperature for magnetic order to disorder.

Based on the detailed characteristic of MT curves, $Tm_{1-x}Ho_xGa$ ($0 \leqslant x \leqslant 1$) compounds can be classified into three types. Taking $Tm_{0.85}Ho_{0.15}Ga$, $Tm_{0.4}Ho_{0.6}Ga$, and $Tm_{0.1}Ho_{0.9}Ga$ compounds as representative samples of the three different types, the ZFC and FC curves are presented in Figs. 2(a)–2(c), respectively. For the samples with low Ho content ($0 \leqslant x < 0.4$), the characteristic of magnetic transitions is almost the same as that reported in TmGa compound [26]. The thermal magnetization curve firstly shows a sudden

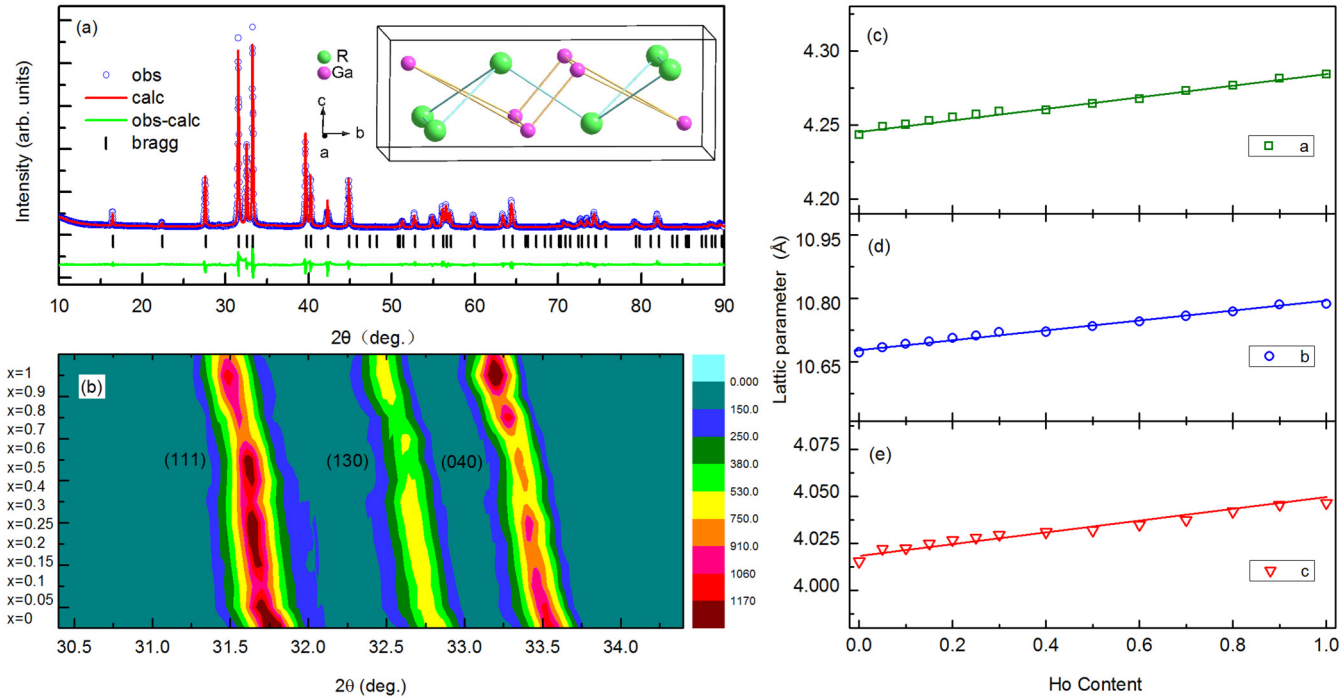

FIG. 1. (a) Rietveld-refined powder XRD pattern of $Tm_{0.4}Ho_{0.6}Ga$ compound at room temperature. Inset is the crystal structure of *R*Ga compound. (b) The contour plot of XRD intensity in a small range of diffraction angle for $Tm_{1-x}Ho_xGa$ ($0 \leqslant x \leqslant 1$) compounds. Ho-content dependences of lattice parameters *a* (c), *b* (d), and *c* (e) for $Tm_{1-x}Ho_xGa$ ($0 \leqslant x \leqslant 1$) compounds.

decrease with increasing temperature and then a peak appears thereafter, which indicates that two magnetic transitions occur successively. It was reported that TmGa undergoes an FM to AFM transition at T_{FA} and an AFM to PM transition at T_N [26] and the incommensurate AFM ground state with the propagation vector $k = (0,\ 0,\ 0.275,\ 0)$ has been confirmed at intermediate temperatures between T_{FA} and T_N according to neutron diffraction experiments [27]. Therefore, the lower transition temperature of $Tm_{1-x}Ho_xGa$ ($0 \leqslant x < 0.4$) compounds is corresponding to T_{FA}, which can be determined from the maximal value of $|dM/dT|$. The higher temperature is corresponding to T_N, which can be determined by the peak position of FC curves. For high Ho content ($0.9 \leqslant x \leqslant 1$), the magnetic transitions are similar to the ones in HoGa compound. With increasing temperature, the magnetization shows a gradual decrease and subsequently a more obvious decrease at two different temperatures, indicating that two magnetic transitions occur. It is known that the two drastic

TABLE I. Magnetic transition temperature and parameters related to magnetocaloric effect under field change of 0–2 T and 0–5 T of $Tm_{1-x}Ho_xGa$ compounds.

				0–2 T			0–5 T		
Samples	T_{SR} (K)	T_{FA} (K)	T_N/T_C (K)	$(-\Delta S_M)_{max}$ (J/kg K)	δT_{FWHM} (K)	RC (J/kg)	$(-\Delta S_M)_{max}$ (J/kg K)	δT_{FWHM} (K)	RC (J/kg)
$x = 0.00$		12.6	15.6	20.3	10.0	138.3	32.3	16.3	381.2
$x = 0.05$		13.4	16.2	17.5	9.5	126.8	28.8	15.8	348.3
$x = 0.10$		14.5	17.0	17.2	11.4	148.6	28.6	17.7	383.8
$x = 0.15$		15.4	17.6	18.0	12.3	168.2	29.6	19.2	434.9
$x = 0.20$		16.2	18.2	15.2	11.7	136.4	26.1	19.3	381.4
$x = 0.25$		16.8	18.6	15.0	14.0	160.6	25.8	21.4	422.1
$x = 0.30$		18.1	19.3	12.6	15.7	147.5	22.4	24.0	409.9
$x = 0.40$	19.8	27.0	31.0	6.6	27.0	177.4	16.3	34.5	477.0
$x = 0.50$	20.3	35.5	38.0	4.6	37.8	209.9	13.4	44.3	519.3
$x = 0.60$	20.8	42.0	44.0	4.6	44.6	219.7	13.2	51.6	553.8
$x = 0.70$	20.4	48.5	50.0	7.5	45.5	182.7	14.5	55.3	543.5
$x = 0.80$	20.4	54.5	55.5	6.0	49.4	117.0	12.3	61.0	393.9
$x = 0.90$	20.3		60.5	3.7	59.9	171.0	10.3	70.3	469.0
$x = 1.00$	20.2		66.5	8.1	60.1	174.1	15.2	70.2	526.3

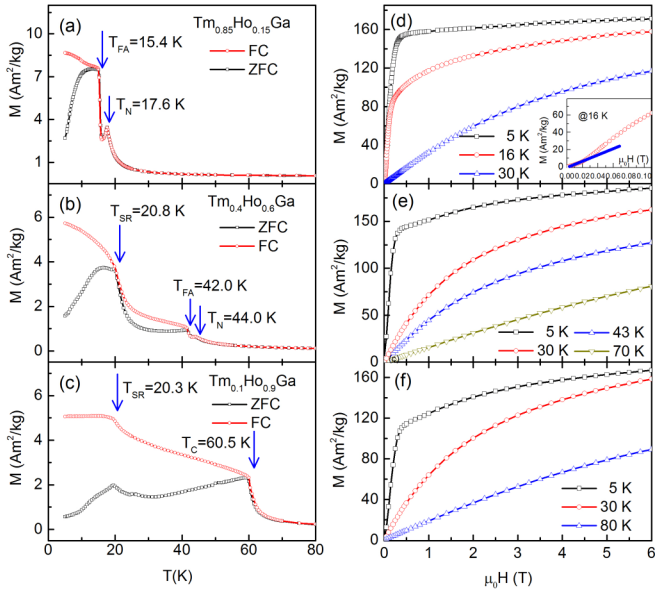

FIG. 2. Temperature dependences of the magnetization with the applied field of 0.01 T for $Tm_{0.85}Ho_{0.15}Ga$ (a), $Tm_{0.4}Ho_{0.6}Ga$ (b), and $Tm_{0.1}Ho_{0.9}Ga$ (c) compounds. Isotherms magnetization curves for $Tm_{0.85}Ho_{0.15}Ga$ (d), $Tm_{0.4}Ho_{0.6}Ga$ (e), and $Tm_{0.1}Ho_{0.9}Ga$ (f) compounds. Inset of (d) shows the isotherms magnetization curve measured at 16 K in low-field range.

changes of HoGa compound correspond to spin reorientation and FM to PM transition, respectively [19,28]. The magnetic transitions have been confirmed by Mössbauer spectroscopy and high-resolution neutron powder-diffraction experiments [19,29,30]. The SR transition originates from the competition between magnetic exchange interaction and the crystal-field interaction. The magnetic moments of Ho atoms cant away from the *ab* plane towards the *c* axis as temperature goes up and exceeds T_{SR} [22]. The transition temperatures of SR and FM to PM transition were marked as T_{SR} and T_C, respectively, as shown in Fig. 2(c). As for the $Tm_{1-x}Ho_xGa$ samples with intermediate Ho content ($0.4 \leqslant x < 0.9$), three successive magnetic transitions were observed as presented in Fig. 2(b). Although the characteristic of MT curve becomes more complex, it can be concluded that these samples undergo an SR transition, an FM to AFM transition, and an AFM to PM transition with increasing temperature based on the other two types of magnetic transitions and the change trend of transition temperatures with Ho content. The magnetic transitions will be discussed further in the following section.

The isothermal magnetization curves as a function of magnetic field (MH) were measured with applied fields up to 6 T for $Tm_{1-x}Ho_xGa$ ($0 \leqslant x \leqslant 1$) compounds. The typical curves of $Tm_{0.85}Ho_{0.15}Ga$, $Tm_{0.4}Ho_{0.6}Ga$, and $Tm_{0.1}Ho_{0.9}Ga$ compounds are presented in Figs. 2(d)–2(f), respectively. It can be seen that the magnetization at 5 K increases rapidly with increasing fields and almost reaches the saturation value with a field of 0.5 T, which is a typical characteristic of FM ground state. The inset of Fig. 2(d) shows the enlarged view of MH curve at 16 K in low-field range for $Tm_{0.85}Ho_{0.15}Ga$ sample. The MH curve at 16 K shows a typical feature of AFM ground state, where the magnetization approximately follows

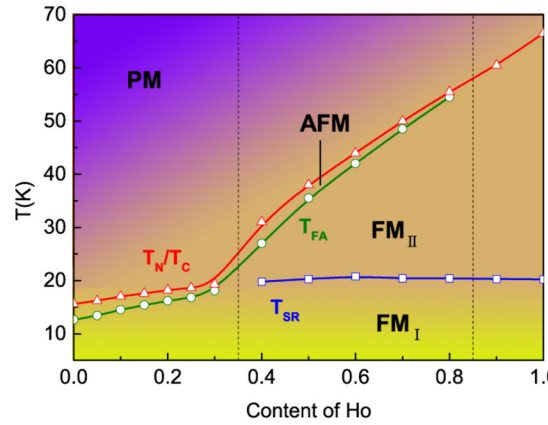

FIG. 3. Magnetic diagram of $Tm_{1-x}Ho_xGa$ ($0 \leqslant x \leqslant 1$) compounds.

a linear relationship with magnetic field at low fields [inset of Fig. 2(d)] and it further increases when the field exceeds a critical value [31]. That is to say, the FM to AFM transition and AFM to PM transition of $Tm_{0.85}Ho_{0.15}Ga$ compound were further confirmed by isothermal magnetization measurement. For most cases, the direction of spontaneous magnetization changes with temperature going through T_{SR}, however the magnetic ground state keeps FM order below and above T_{SR} [19,28]. For $Tm_{0.4}Ho_{0.6}Ga$ sample, the MH curves shown in Fig. 2(e) indicate that the magnetic ground states at 5 and 30 K are both FM, which is in good accordance with the nature of SR transition. Based on the description of magnetic transitions, the ground state of $Tm_{0.4}Ho_{0.6}Ga$ compound at 43 K is AFM. However, no obvious characteristic of AFM was observed on the MH curve at 43 K, because the AFM ground state becomes weaker and weaker with the AFM temperature zone shrinking. As for $Tm_{0.1}Ho_{0.9}Ga$ compound shown in Fig. 2(f), the ground state of FM order was observed both below and above T_{SR}, which is similar to the reported results of HoGa compound [22,25].

All of the transition temperatures of $Tm_{1-x}Ho_xGa$ ($0 \leqslant x \leqslant 1$) compounds are listed in Table I. Moreover, the magnetic phase diagram of $Tm_{1-x}Ho_xGa$ ($0 \leqslant x \leqslant 1$) compounds is presented in Fig. 3. The order to disorder transition temperatures including T_N and T_C were analyzed before and the monotonous variation tendency were discussed. According to Table I, the value of T_{FA} also shows an obvious monotonic increase from 12.6 K ($x = 0$) to 54.5 K ($x = 0.8$). For $Tm_{1-x}Ho_xGa$ ($0 \leqslant x \leqslant 1$) compounds, the FM to AFM transition originates from the competition between FM and AFM order. It was found that incommensurate modulated AFM order exists in TmGa compound, but no AFM ground state exists in HoGa compound, indicating that Ho atoms are inclined to couple with FM order while Tm atoms tend to AFM order in *R*Ga crystal structure. Therefore, with increasing Ho content, FM order is enhanced and the value of T_{FA} goes up steadily. Meanwhile, it should be noticed that Ho substitution will bring in another order to order transition known as SR transition according to the magnetic properties of HoGa compound [22]. It was found that SR transition exists in the $Tm_{1-x}Ho_xGa$ samples with $0.4 \leqslant x \leqslant 1$ and the value of T_{SR} shows a rather different variation tendency compared

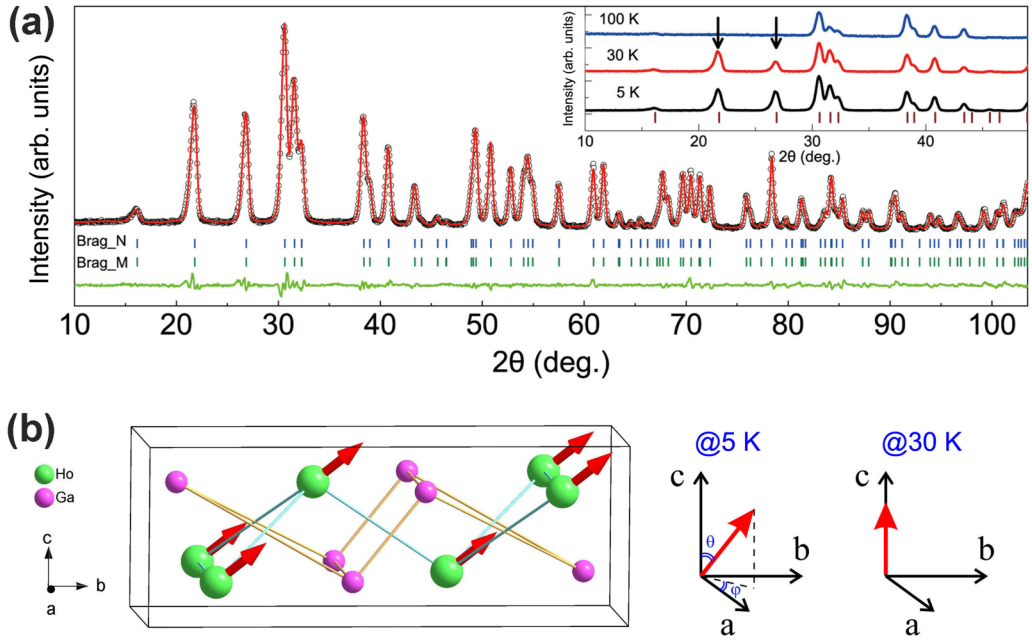

FIG. 4. (a) The refinement of neutron powder-diffraction pattern of $Tm_{0.1}Ho_{0.9}Ga$ compound at 5 K ($R_B = 1.96\%$, $R_F = 1.26\%$, $R_M = 1.57\%$, $\chi^2 = 5.03$). The inset shows the NPD data at 5, 30, and 100 K, respectively. The arrows are corresponding to the Bragg positions of the magnetic contribution. (b) The magnetic structure of $Tm_{0.1}Ho_{0.9}Ga$ compound at 5 K and the schematic plots of the direction of FM order below and above T_{SR}.

with T_N/T_C and T_{FA}. Specifically speaking, T_{SR} is about 20.0 K with a little variation with the changing of Ho content. In fact, SR transition results from the competition between magnetic exchange interaction and crystal-field interaction [19]. On one hand, the magnetic exchange interaction only shows relatively small variation because the adjacent atomic numbers are close to each other for $Tm_{1-x}Ho_xGa$ ($0.4 \leqslant x \leqslant 1$) compounds. On the other hand, the interaction of crystal field correlates with crystal symmetry and atomic surroundings in *R*-based compounds [13,14]. $Tm_{1-x}Ho_xGa$ ($0 \leqslant x \leqslant 1$) compounds have been confirmed to have uniform crystal structure and close atomic coordinates, indicating that the rare-earth atoms have the similar circumstance. As a result, the value of T_{SR} shows a negligible change with increasing Ho content. In fact, this kind of characteristic of T_{SR} has been reported in other *R*Ga compounds such as $Gd_xEr_{1-x}Ga$ compounds [13].

In order to further investigate the specific form of SR transition and magnetic structure of $Tm_{1-x}Ho_xGa$ compounds, neutron powder diffraction (NPD) experiments of $Tm_{0.1}Ho_{0.9}Ga$ compound were carried out at 5, 17, 30, 50, 100, and 300 K, respectively, and the NPD patterns at 5, 30, and 100 K are presented in the inset of Fig. 4(a). The Bragg peaks at 100 K only come from the nuclear contribution while the Bragg peaks at 5 and 30 K contain not only the contributions of nucleus but also the contributions of magnetic moments. The extra magnetic peaks at 5 and 30 K are marked with arrows as shown in the inset of Fig. 4(a). It should be noted that all of the magnetic peaks can be indexed to the nuclear structure, indicating that the magnetic Ho/Tm sublattice has the same symmetry with crystal structure in $Tm_{0.1}Ho_{0.9}Ga$ compound and simple ferromagnetic order exists. All the NPD patterns were fitted with Rietveld method and the refinement at 5 K was shown in Fig. 4(a). Since no signal of superlattice was observed, crystal structure with *Cmcm* space group and magnetic structure with propagation vector of (0, 0, 0) were used. The errors were calculated as $R_B = 1.96\%$, $R_F = 1.26\%$, $R_M = 1.57\%$, and $\chi^2 = 5.03$. The magnetic structure at 5 K based on refinement is shown in Fig. 4(b) and it was found that three ferromagnetic components all exist with $M_x = 3.4(1)\,\mu_B$, $M_y = 3.1(2)\,\mu_B$, and $M_z = 7.29(8)\,\mu_B$. Furthermore, the magnetic structures at other temperatures were also resolved and the detailed results together with other refined parameters are all presented in Table II. It can be seen that not only the value of magnetic moment but also the direction of FM order changes with increasing temperature. Three components of FM order all exist at the temperatures below T_{SR}, but only the component of M_z can be observed above T_{SR}. The schematic plots of the direction of FM order at 5 and 30 K are also shown in Fig. 4(b). That is to say, the zenith angle of the magnetic moment in $Tm_{0.1}Ho_{0.9}Ga$ compound changes from nonzero value to zero value during the processing of SR transition as temperature goes up, which is similar to the SR transition of HoGa compound [22]. The SR transition is related to the asymmetric electron cloud of Tm/Ho atoms and atomic surroundings and it results from the competition between magnetic exchange interaction and the crystal-field effect interaction [19].

The behavior of magnetic entropy change of $Tm_{1-x}Ho_xGa$ ($0 \leqslant x \leqslant 1$) compounds was investigated and the values of ΔS_M were calculated based on isothermal magnetization data by using the Maxwell relation $\Delta S_M = \int_0^H (\partial M/\partial T)_H dH$ [32]. The temperature dependences of ΔS_M under field change of 0–2 T and 0–5 T are shown in Figs. 5(a)–5(c) for $Tm_{0.85}Ho_{0.15}Ga$, $Tm_{0.4}Ho_{0.6}Ga$, and $Tm_{0.1}Ho_{0.9}Ga$ samples, respectively. Although $Tm_{0.85}Ho_{0.15}Ga$ compound undergoes two magnetic transitions, only one peak can be observed on

TABLE II. Refined structure parameters of $Tm_{0.1}Ho_{0.9}Ga$. Space group *Cmcm*. Atomic position: Tm/Ho, 4*c* (0, *y*, 0.25); Ga, 4*c* (0, *y*, 0.25).

Parameters		5 K	17 K	30 K	50 K	100 K	300 K
a (Å)		4.272 61(8)	4.271 99(8)	4.272 07(9)	4.272 50(9)	4.272 0(1)	4.275 8(1)
b (Å)		10.738 8(2)	10.739 4(2)	10.740 2(2)	10.740 3(2)	10.738 5(2)	10.767 0(3)
c (Å)		4.0281 3(8)	4.028 62(8)	4.028 7(1)	4.029 40(9)	4.029 11(9)	4.040 2(1)
V (Å^3)		184.822(6)	184.828(6)	184.849(7)	184.901(7)	184.836(8)	186.007(8)
Tm/Ho	*y*	0.3598 2(7)	0.3598 3(8)	0.360 0(1)	0.360 0(1)	0.359 9(1)	0.359 7(1)
	M_x (μ_B)	3.4 (1)	0.7(5)	0	0		
	M_y (μ_B)	3.1 (2)	3.0(2)	0	0		
	M_z (μ_B)	7.29(8)	7.52(7)	7.35(5)	5.83(4)		
	M (μ_B))	8.7(1)	8.1(1)	7.35(5)	5.83(4)		
	θ (deg)	32.5(9)	22(1)	0	0		
	φ (deg)	42(2)	77(9)				
Ga	*y*	0.075 2(2)	0.075 3(2)	0.075 3(2)	0.07 53(2)	0.075 5(1)	0.075 7(1)
R_B (%)		1.96	2.23	2.91	2.45	2.61	3.13
R_F (%)		1.26	1.40	1.94	1.76	1.91	2.40
R_M (%)		1.57	1.76	2.91	2.47		
χ^2		5.03	4.85	6.35	4.32	2.05	4.31

the ΔS_M curve as shown in Fig. 5(a). This is because the FM to AFM and AFM to PM transition are so close to each other that the two kinds of contributions to ΔS_M are merged together. The ΔS_M curve of $Tm_{0.85}Ho_{0.15}Ga$ compound is similar to that of TmGa compound [26]. As for $Tm_{0.4}Ho_{0.6}Ga$ compound shown in Fig. 5(b), two peaks can be obviously observed on the ΔS_M curve. The peak at lower temperature comes from SR transition and the peak at higher temperature contains contributions from both FM to AFM transition and AFM to PM transition. When $x = 0.9$, there are two peaks [see Fig. 5(c)] and they originate from SR transition and FM to PM transition, respectively, which is in accordance with expectation. It should also be noted that the peak value at lower temperature is larger than that at higher temperature both for $Tm_{0.4}Ho_{0.6}Ga$ and $Tm_{0.1}Ho_{0.9}Ga$ compounds, indicating that the changing of magnetic order during SR transition is fiercer than that during FM to PM transition. Actually, the peak overlap on ΔS_M curves exists for the $Tm_{1-x}Ho_xGa$ samples with Ho content less than 0.4. In order to further analyze the feature of MCE peaks, the critical exponent *n* was investigated according to $|\Delta S_M| \propto H^n$ [33] and the temperature dependences of *n* for $Tm_{0.85}Ho_{0.15}Ga$, $Tm_{0.4}Ho_{0.6}Ga$, and $Tm_{0.1}Ho_{0.9}Ga$ compounds are shown in Figs. 5(d)–5(f), respectively. The magnitude of magnetic field used here is 6 T. It can be seen that the *n*-*T* curves described the two overlapped MCE peaks with more details. There is a small

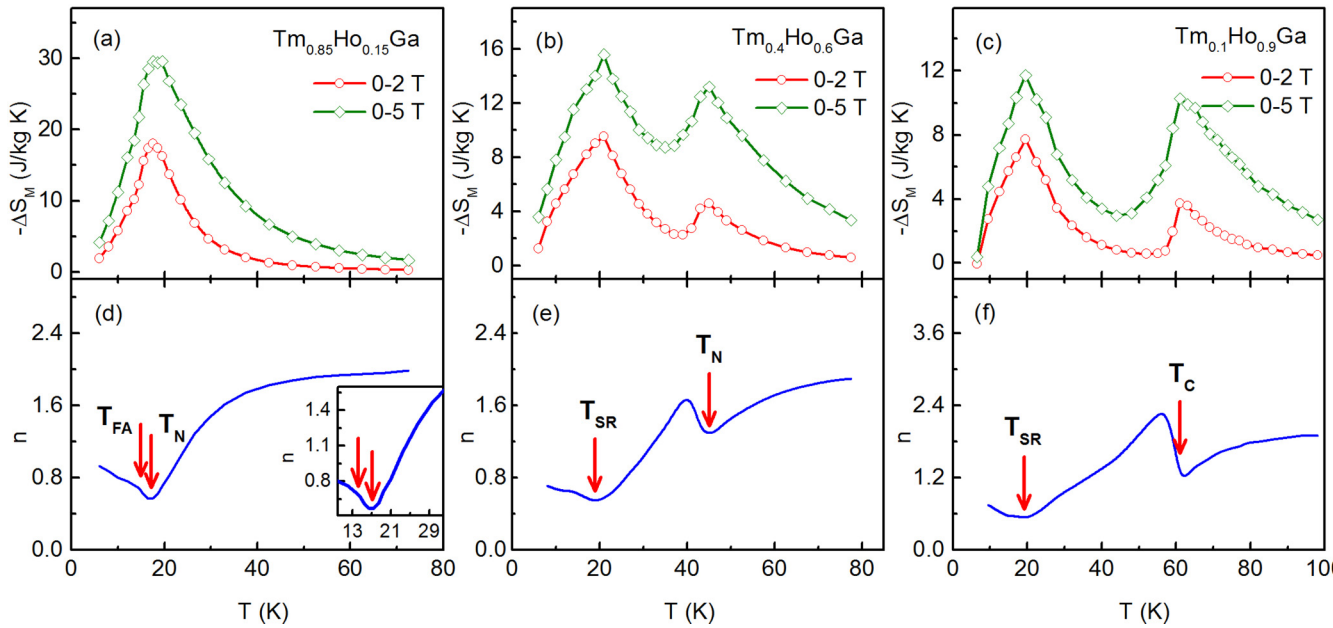

FIG. 5. Temperature dependences of magnetic entropy change under field change of 0–2 T and 0–5 T for $Tm_{0.85}Ho_{0.15}Ga$ (a), $Tm_{0.4}Ho_{0.6}Ga$ (b), and $Tm_{0.1}Ho_{0.9}Ga$ (c), respectively. The Ho-content dependence of critical exponent *n* for $Tm_{0.85}Ho_{0.15}Ga$ (d), $Tm_{0.4}Ho_{0.6}Ga$ (e), and $Tm_{0.1}Ho_{0.9}Ga$ (f), respectively.

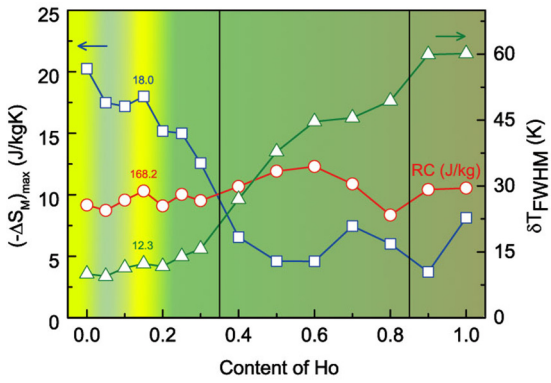

FIG. 6. The composition dependence of $(-\Delta S_M)_{max}$, δT_{FWHM}, and RC for $Tm_{1-x}Ho_xGa$ ($0 \leqslant x \leqslant 1$) compounds under field change of 0–2 T.

bulge corresponding to T_{FA} and a minimum around T_N on the n-T curves for $Tm_{0.85}Ho_{0.15}Ga$ compound. Furthermore, two minimal values are observed on the n-T curves corresponding to T_{SR} and T_N/T_C, respectively, for the $Tm_{1-x}Ho_xGa$ compounds with more Ho concentrations. Additionally, there is no observation for overshoot of $n > 2$ around transition temperatures, indicating second-order magnetic transitions [34,35].

The detailed magnetic parameters of $Tm_{1-x}Ho_xGa$ ($0 \leqslant x \leqslant 1$) compounds including transition temperatures, $(-\Delta S_M)_{max}$ around T_N or T_C, δT_{FWHM}, and RC value are listed in Table I. Besides, the composition dependence of MCE parameters for 0–2 T is shown in Fig. 6. To evaluate MCE materials, ΔS_M is usually the primary consideration and δT_{FWHM} together with RC is the necessary supplemental description. Generally to say, the value of $(-\Delta S_M)_{max}$ exceeds 12.0 and 22.0 J/kg K under 0–2 T and 0–5 T, respectively, for the $Tm_{1-x}Ho_xGa$ compounds with $0 \leqslant x < 0.4$, indicating that large MCE is obtained at low temperatures around liquid hydrogen temperature compared with $Er_{12}Co_7$ (10.2 and 18.3 J/kg K for 0–2 T and 0–5 T at 13.6 K) and GdNiBC (9.3 and 19.8 J/kg K for 0–2 T and 0–5 T at 15.0 K) compounds, respectively [36,37]. Especially, it is found that $(-\Delta S_M)_{max}$ firstly increases from 17.5 J/kg K for $x = 0.05$ to 18.0 J/kg K for $x = 0.15$ under 0–2 T, then it drops when x is larger than 0.15. Therefore, the value of $(-\Delta S_M)_{max}$ shows a local maximum at $x = 0.15$ for $Tm_{1-x}Ho_xGa$ ($0 \leqslant x \leqslant 1$) compounds as Ho content varies. In fact, $(-\Delta S_M)_{max}$ is located around the order to disorder transition temperature, which obeys the following relationship [38]:

$$(-\Delta S_M)_{max} \approx 1.07nR\left(\frac{g\mu_B JH}{kT_0}\right), \quad (1)$$

where n is the number of magnetic ions per mole, R is the gas constant, g is the Landé factor, μ_B is the Bohr magneton, J is the total angular momentum quantum number, H is magnetic field, k is the Boltzmann constant, and T_0 is order to disorder transition temperatures (T_N or T_C), respectively. With respect to $Tm_{1-x}Ho_xGa$ series, the variation of Ho content is accompanied by the change of J and T_0. On one hand, it has been discussed that T_0 goes up with increasing Ho content. On the other hand, the average value of J also increases with Ho content because J of Ho atoms is larger than that of Tm atoms. Therefore it is difficult to give a detailed and precise prediction of variation trend on $(-\Delta S_M)_{max}$ with changing Ho content. As a result, the value of $(-\Delta S_M)_{max}$ shows a rough decrease trend on the whole and a local increase for several kinds of component with increasing Ho content according to Fig. 6. When the content of Ho is 15%, the value of $(-\Delta S_M)_{max}$ together with δT_{FWHM} and RC all show a local maximum. It is notable that 15% of Ho substitution does not bring any increase on $(-\Delta S_M)_{max}$ of TmGa compound. However, an obvious improvement on δT_{FWHM} and RC was obtained. For example, the value of δT_{FWHM} and RC under 0–2 T for $Tm_{0.85}Ho_{0.15}Ga$ compound shows enhancement of 23.0 and 21.6% compared with TmGa compound, correspondingly. The value of δT_{FWHM} and RC under 0–5 T shows enhancement of 17.8 and 14.1% compared with TmGa compound, correspondingly. That is to say, $Tm_{0.85}Ho_{0.15}Ga$ compound shows better MCE performance than TmGa compound, because large $(-\Delta S_M)_{max}$ together with balanced δT_{FWHM} and RC is usually expected for excellent MCE materials. The improvement on MCE results from the optimization of spin and orbital quantum number by Ho substitution.

IV. CONCLUSIONS

In summary, Ho substitution has a large influence on the magnetic exchange interactions between rare-earth atoms in $Tm_{1-x}Ho_xGa$ compounds, which further affects the magnetic transitions and MCE. The systematic study indicates that three types of successive magnetic transitions exist for $Tm_{1-x}Ho_xGa$ compounds with increasing temperature, and the SR transition in $Tm_{0.1}Ho_{0.9}Ga$ compound was investigated in detail according to neutron powder-diffraction experiments. Several $Tm_{1-x}Ho_xGa$ compounds with large $(-\Delta S_M)_{max}$ more than 12.0 and 22.0 J/kg K under 0–2 T and 0–5 T were obtained. Particularly, $Tm_{0.85}Ho_{0.15}Ga$ compound shows best-balanced MCE performance among them. Besides large $(-\Delta S_M)_{max}$, $Tm_{0.85}Ho_{0.15}Ga$ compound has a δT_{FWHM} of 12.3 K and RC of 168.2 J/kg under field change of 0–2 T showing enhancement of 23.0 and 21.6%, correspondingly, compared with TmGa compound. This work indicates that Ho substitution on the basis of S or J optimization is an effective way to manipulate the magnetic transitions and MCE of $Tm_{1-x}Ho_xGa$ compounds.

ACKNOWLEDGMENTS

This work was supported by the National Key Research and Development Program of China (Grants No. 2017YFB0702701, No. 2019YFB2005800, No. 2017YFA0206300, and No. 2017YFA0403701), the National Natural Science Foundation of China (Grants No. 51871019, No. 11674008, No. 51590880, No. 51625101, No. 51971026, No. 51701130, No. 51731001, and No. 51961145305), 111 project (Project No. B170003), and Key Program of the Chinese Academy of Sciences (Grants No. 112111KYSB20180013 and No. QYZDY-SSW-SLH020).

[1] E. Brück, N. T. Trung, Z. Q. Ou, and K. H. J. Buschow, Scr. Mater. **67**, 590 (2012).

[2] F. Guillou, H. Yibole, N. H. van Dijk, L. Zhang, V. Hardy, and E. Brück, J. Alloys Compd. **617**, 569 (2014).

[3] V. Franco, J. S. Blázquez, J. J. Ipus, J. Y. Law, L. M. Moreno-Ramírez, and A. Conde, Prog. Mater. Sci. **93**, 112 (2018).

[4] V. Franco, J. S. Blázquez, B. Ingale, and A. Conde, Ann. Rev. Mater. Res. **42**, 305 (2012).

[5] L. Mañosa and A. Planes, Adv. Mater. **29**, 1603607 (2017).

[6] M. Balli, S. Jandl, P. Fournier, and A. Kedous-Lebouc, Appl. Phys. Rev. **4**, 021305 (2017).

[7] X. Moya, S. Kar-Narayan, and N. D. Mathur, Nat. Mater. **13**, 439 (2014).

[8] A. M. Tishin and Y. I. Spichkin, Int. J. Refrig. **37**, 223 (2014).

[9] Q. Y. Dong, B. G. Shen, J. Chen, J. Shen, and J. R. Sun, J. Appl. Phys. **105**, 113902 (2009).

[10] B. Li, W. J. Hu, X. G. Liu, F. Yang, W. J. Ren, X. G. Zhao, and Z. D. Zhang, Appl. Phys. Lett. **92**, 242508 (2008).

[11] P. J. von Ranke, V. K. Pecharsky, and K. A. Gschneidner, Phys. Rev. B **58**, 12110 (1998).

[12] L. Li and M. Yan, J. Alloys Compd. **823**, 153810 (2020).

[13] X. Q. Zheng, J. Chen, L. C. Wang, R. R. Wu, F. X. Hu, J. R. Sun, and B. G. Shen, J. Appl. Phys. **115**, 17A905 (2014).

[14] X. Q. Zheng, B. Zhang, H. Wu, F. X. Hu, Q. Z. Huang, and B. G. Shen, J. Appl. Phys. **120**, 163907 (2016).

[15] Y. Liu, L. Xu, Q. Wang, W. Li, and X. Zhang, Appl. Phys. Lett. **94**, 172502 (2009).

[16] S. A. Nikitin, K. P. Skokov, Y. S. Koshkid'ko, Y. G. Pastushenkov, and T. I. Ivanova, Phys. Rev. Lett. **105**, 137205 (2010).

[17] A. Biswas, N. A. Zarkevich, A. K. Pathak, O. Dolotko, I. Z. Hlova, A. V. Smirnov, Y. Mudryk, D. D. Johnson, and V. K. Pecharsky, Phys. Rev. B **101**, 224402 (2020).

[18] M. M. Piva, R. Tartaglia, G. S. Freitas, J. C. Souza, D. S. Christovam, S. M. Thomas, J. B. Leão, W. Ratcliff, J. W. Lynn, C. Lane, J. X. Zhu, J. D. Thompson, P. F. S. Rosa, C. Adriano, E. Granado, and P. G. Pagliuso, Phys. Rev. B **101**, 214431 (2020).

[19] N. N. Delyagin, V. I. Krylov, and I. N. Rozantsev, J. Magn. Magn. Mater. **308**, 74 (2007).

[20] R. A. Susilo, J. M. Cadogan, D. H. Ryan, N. R. Lee-Hone, R. Cobas, and S. Muñoz-Pérez, Hyperfine Interact. **226**, 257 (2014).

[21] R. A. Susilo, J. M. Cadogan, S. Muñoz-Pérez, R. Cobas, W. D. Hutchison, and M. Avdeev, J. Magn. Magn. Mater. **390**, 36 (2015).

[22] R. A. Susilo, S. M. Pérez, R. Cobas, J. M. Cadogan, and M. Avdeev, J. Phys.: Conf. Ser. **340**, 012071 (2012).

[23] N. Shohata, J. Phys. Soc. Jpn. **42**, 1873 (1977).

[24] X. Q. Zheng and B. G. Shen, Chin. Phys. B **26**, 027501 (2017).

[25] J. Chen, B. G. Shen, Q. Y. Dong, and J. R. Sun, Solid State Commun. **150**, 157 (2010).

[26] Z. J. Mo, J. Shen, L. Q. Yan, C. C. Tang, J. Lin, J. F. Wu, J. R. Sun, L. C. Wang, X. Q. Zheng, and B. G. Shen, Appl. Phys. Lett. **103**, 052409 (2013).

[27] J. M. Cadogan, G. A. Stewart, S. Munoz Perez, R. Cobas, B. R. Hansen, M. Avdeev, and W. D. Hutchison, J. Phys.: Condens. Matter **26**, 116002 (2014).

[28] J. Chen, B. G. Shen, Q. Y. Dong, F. X. Hu, and J. R. Sun, Appl. Phys. Lett. **95**, 132504 (2009).

[29] K. Y. Wang, M. Sawicki, K. W. Edmonds, R. P. Campion, S. Maat, C. T. Foxon, B. L. Gallagher, and T. Dietl, Phys. Rev. Lett. **95**, 217204 (2005).

[30] Y. Liu, L. Peng, J. Zhang, Z. Ren, J. Yang, Z. Yang, S. Cao, and W. Fang, Europhys. Lett. **96**, 27015 (2011).

[31] J. Chen, B. G. Shen, Q. Y. Dong, F. X. Hu, and J. R. Sun, Appl. Phys. Lett. **96**, 152501 (2010).

[32] V. K. Pecharsky and K. A. Gschneidner, Phys. Rev. Lett. **78**, 4494 (1997).

[33] V. Franco, A. Conde, V. K. Pecharsky, and K. A. Gschneidner, Europhys. Lett. (EPL) **79**, 47009 (2007).

[34] V. Franco, J. S. Blázquez, and A. Conde, Appl. Phys. Lett. **89**, 222512 (2006).

[35] J. Y. Law, V. Franco, L. M. Moreno-Ramirez, A. Conde, D. Y. Karpenkov, I. Radulov, K. P. Skokov, and O. Gutfleisch, Nat. Commun. **9**, 2680 (2018).

[36] X. Q. Zheng, B. Zhang, Y. Q. Li, H. Wu, H. Zhang, J. Y. Zhang, S. G. Wang, Q. Z. Huang, and B. G. Shen, J. Alloys Compd. **680**, 617 (2016).

[37] L. Li, M. Kadonaga, D. Huo, Z. Qian, T. Namiki, and K. Nishimura, Appl. Phys. Lett. **101**, 122401 (2012).

[38] H. Oesterreicher and F. T. Parker, J. Appl. Phys. **55**, 4334 (1984).